Gas Physics With Grid-based Codes

Philipp Girichidis

23 January 2014

Preface

Here is one general remark for the participants in the Cosmology lecture series: This lecture is not about a cosmological topic. The lecture captures gas physics with a focus on the numerical solutions. There might be cosmological applications but I don't work in this field and can only contribute with non-cosmological and/or general problems in gas physics.

Literature

Here are a few books/articles that I can recommend (not ordered)

- Most of the first part follows the book by Randall J. Leveque: *Finite Volume Methods for Hyperbolic Problems*, Cambridge University Press, 2002, 2006. The book gives a good general introduction to all details of the equations in general (e.g., linear vs. non-linear), not directly related to astrophysics
- The book by Eleutorio Toro, *Riemann Solvers and Numerical Methods for Fluid Dynamics*, Springer 2009, starts with the Euler equations and contains more technical details and more details about individual solver models and implementations.
- A general introduction is given in Leveque, Mihalas, Dorfi, Müller, *Computational Methods for Astrophysical Fluid Flow*, Springer 1998. This book also covers radiation hydrodynamics and a bit of magnetic fields, but is much less technical.
- An excellent introduction to magnetic fields in astrophysics is given in Spruit, *Essential Magnetohydrodynamics for Astrophysics*, (arXiv:1301.5572).

Contents

1 Introduction

- This lecture is primarily concerned with the solution to gas dynamics.
- Gas is treated as a fluid: *hydrodynamics*
- primary assumption: mean free path of particles is much smaller than the computational resolution element
- This assumption seems natural, however, in relativistic gas flows or jets this assumption might be easily violated. In the presence of magnetic fields (strong magnetic fields) the gyration of the high energy particles (charged / ionised) leads to an effective mean free path smaller than the computational cell and the hydrodynamic approach is again justified.
- fluid equations: *Navier-Stokes equation* (includes viscosity and heat conduction) or the linear simplification, *Euler equations*
- Euler equations capture shock waves and discontinuities in the solution even from very smooth initial conditions.
- shocks and discontinuities have typical length scales much smaller than the resolution element
- micro-physics cannot be modelled
- focus on sophisticated solvers in order to capture the "correct" macroscopic behaviour with "insufficient" resolution
- naive discretisations may easily result in smeared-out representation of shocks or else produce oscillations near discontinuities

2 Classes of Partial Differential Equations

2.1 Classification

- consider the linear PDE in two variables

$$a\,\frac{\partial^2 u}{\partial x^2} + b\,\frac{\partial^2 u}{\partial x \partial y} + c\,\frac{\partial^2 u}{\partial y^2} + d\,\frac{\partial u}{\partial x} + e\,\frac{\partial u}{\partial y} + f\,u = g \tag{2.1}$$

  This equation is linear because all derivatives appear linearly.

- use common notation $u_x = \frac{\partial u}{\partial x}$, $u_{xx} = \frac{\partial^2 u}{\partial x^2}$, ...
- example of a simple non-linear PDE: Burgers equation

$$u_t + u\,u_x = 0 \tag{2.2}$$

- Classification (based on similarity to conic sections): define

$$D = ac - \left(\frac{b(x,y)}{2}\right)^2 \tag{2.3}$$

  - $D > 0$: elliptical
  - $D = 0$: parabolic
  - $D < 0$: hyperbolic

- only coefficient functions of highest derivatives are considered
- coefficients can be functions $a = a(x, y)$, so type of the PDE depends on position

2.2 Examples

- Laplace / Poisson equation

$$\Delta u = g, \qquad u_{xx} + u_{yy} = 0 \tag{2.4}$$

- $a = c$, $b = 0$, $D > 0$, elliptical
- heat equation

$$u_t - k\, u_{xx} = g \tag{2.5}$$

- $a = b = 0$, $c = k$, $d = -1$, $e = f = 0$, $D = 0$, parabolic
- wave equation

$$u_{tt} - u_{xx} = 0 \tag{2.6}$$

- $a = 1$, $c = -1$, $b = d = e = f = 0$, $D < 0$, hyperbolic

2.3 Generalisation

- alternative definition of the classification scheme based on properties of the of the *coefficient matrix*

$$A(x, y) := \begin{pmatrix} a(x,y) & \frac{b(x,y)}{2} \\ \frac{b(x,y)}{2} & c(x,y) \end{pmatrix} \tag{2.7}$$

  - $A(x, y)$ positive definite or negative definite: "elliptical" at point (x, y)
  - $A(x, y)$ positive semidefinite or negative semidefinite, but not definite (singular): "parabolic" at (x, y)
  - $A(x, y)$ indefinite (with exactly one negative eigenvalue): "hyperbolic" at (x, y)

3 Derivation of Conservation Laws

- consider the simple case of a pipe with a gas or fluid moving at a known speed $u(x, t)$, depending only on the position and the time.
- set q be the concentration of a *tracer* substance, without dynamical effect on the fluid.
- total mass of the tracer, M_t, in the pipe between x_1 and x_2:

$$M_\mathrm{t} = \int_{x_1}^{x_2} q(x, t)dx \tag{3.1}$$

- mass changes only due to inflow and outflow at the beginning and end of the pipe, i.e., flux through the boundaries, $F_{1,2}(t)$, which gives the *integral form* of the conservation law

$$\frac{d}{dt} \int_{x_1}^{x_2} q(x, t)dx = F_1(t) - F_2(t) \tag{3.2}$$

- Note that $+F_1(t)$ and $-F_2(t)$ both represent fluxes *into* the section of the pipe.
- flux at a given point x at time t is simply given by the product

$$\text{flux at } (x, t) = u(x, t)q(x, t) \tag{3.3}$$

or, as $u(x, t)$ is a known function

$$\text{flux } = f(q, x, t) = u(x, t)q \tag{3.4}$$

in the simple case of $u(x, t) = \overline{u}$ (*autonomous* system)

$$\text{flux } = f(q, x, t) = \overline{u}q \tag{3.5}$$

- for general autonomous flux we can rewrite the conservation law as follows

$$\frac{d}{dt}\int_{x_1}^{x_2} q(x,t)dx = f(q(x_1,t)) - f(q(x_2,t)) = -f(q(x,t))\Big|_{x_1}^{x_2} \tag{3.6}$$

- to simplify the search for a solution, transform the system into a partial differential equation and assume that the functions $q(x,t)$ and $f(q)$ are sufficiently smooth in a mathematical sense

$$\frac{d}{dt}\int_{x_1}^{x_2} q(x,t)dx = \int_{x_1}^{x_2} \frac{\partial}{\partial x} f(q(x,t))dx \tag{3.7}$$

$$\int_{x_1}^{x_2} \left[\frac{\partial}{\partial t} q(x,t) + \frac{\partial}{\partial x} f(q(x,t))\right] dx = 0 \tag{3.8}$$

- since this integral must be zero for all values of x_1 and x_2, the integrand needs to be identically zero and we end up with

$$\frac{\partial}{\partial t} q(x,t) + \frac{\partial}{\partial x} f(q(x,t)) = 0 \tag{3.9}$$

which is

$$q_t(x,t) + f(q(x,t))_x = 0 \tag{3.10}$$

3.1 Advection equation

- for the flux with constant velocity (Eq. (3.5)) the conservation law becomes

$$q_t + \overline{u} q_x = 0, \tag{3.11}$$

which is the *advection equation*, a scalar, linear, constant-coefficient PDE of hyperbolic type. The general solution is easy to find. Any smooth function of the form

$$q(x,t) = \tilde{q}(x - \overline{u}t) \tag{3.12}$$

satisfies the differential equation (3.11). Here, $q(x,t)$ is constant along any ray in space-time for which $x - \overline{u}t$ is constant, i.e., all along rays $X(t) = x_0 + \overline{u}t$ the value of $q(X(t),t) = \tilde{q}(x_0)$. These rays are the *characteristics* of the equation. Along characteristics, the equations simplify (see figure 1):

$$\frac{d}{dt} q(X(t),t) = q_t(X(t),t) + X'(t) q_x(X(t),t) \tag{3.13}$$

$$= q_t + \overline{u} q_x \tag{3.14}$$

$$= 0 \tag{3.15}$$

q is constant along characteristics. The concept of the characteristics is fundamental and plays an important role in the development of hydro solvers.

- To find a particular solution we need *initial conditions* and *boundary conditions*. Use the initial value

$$q(x,t_0) = \mathring{q}(x) \tag{3.16}$$

Since the value of q must be constant along characteristics, we find that

$$q(x,t) = \mathring{q}(x - \overline{u}(t - t_0)), \tag{3.17}$$

the initial profile simply translates with speed $\overline{u}$.

- If the pipe has finite length, we need to specify the density of the tracer entering the pipe at one end, depending on the velocity. For $\overline{u} > 0$ we specify the value at the left boundary $x = a$

$$q(a,t) = g_0(t) \tag{3.18}$$

and we end up with the solution

$$q(x,t) = \begin{cases} g_0(t - (x-a)/\overline{u}) & \text{if } a < x < a + \overline{u}(t - t_0) \\ \mathring{q}(x - \overline{u}(t - t_0)) & \text{if } a + \overline{u}(t - t_0) < x < b \end{cases} \tag{3.19}$$

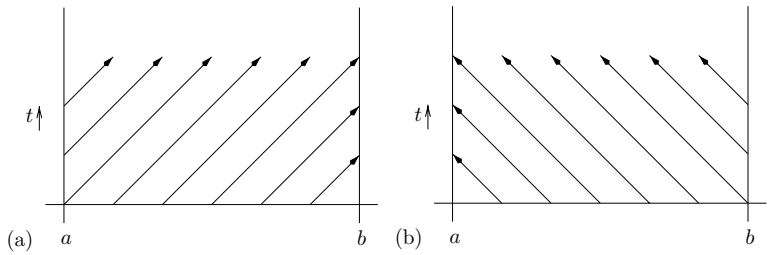

Figure 1: Solutions to the advection equation is constant along the characteristics, shown for (a) $\overline{u} > 0$ and (b) $\overline{u} < 0$.

3.2 Variable Coefficients

If the fluid velocity u varies with x then the conservation law reads

$$q_t + (u(x)q)_x = 0 \tag{3.20}$$

In this case the characteristic curves $X(t)$ are solutions to the *ordinary differential equations*

$$X'(t) = u(X(t)) \tag{3.21}$$

Along the characteristic curve we find that the advection equation simplifies to

$$\begin{aligned}
\frac{d}{dt}q(X(t),t) &= q_t(X(t),t) + X'(t)q_x(X(t),t) && (3.22)\\
&= q_t + u(X(t))q_x && (3.23)\\
&= q_t + (u(X(t))q)_x - u'(X(t))q && (3.24)\\
&= -u'(X(t))q(X(t),t). && (3.25)
\end{aligned}$$

This means when u is no longer constant then the characteristics are no longer straight lines and the solution q is no longer constant along the curves. The operator $\partial_t + u\partial_x$ is called *material derivative* since it represents the differentiation along the characteristic curve and computes the rate of change observed by a material particle moving with the fluid.

Note the difference to the non-conserving advection equation

$$q_t + u(x)q_x = 0, \tag{3.26}$$

for which equation (3.23) is zero, so that q is constant along characteristic curves. Which equation applies depends on the physical quantity and the units in which the equations are measured. For a concentration in $\mathrm{g\,cm^{-1}}$ we have equation (3.20), a density in $\mathrm{g\,cm^{-3}}$ leads to equation (3.26).

3.3 Diffusion and the Advection-Diffusion Equation

According to *Fick's law of diffusion* the net flux is proportional to the *gradient* of q

$$\text{flux of } q = f(q_x) = -\beta q_x, \tag{3.27}$$

with β being the diffusion coefficient. Using this relation in the differential equation of the conservation law (Eq. 3.9) gives the *diffusion equation*

$$q_t = \beta q_{xx}. \tag{3.28}$$

In many astrophysical applications the diffusion coefficient varies (diffusion of radiation (FLD), diffusion of CRs along magnetic field lines, thermal diffusion for different chemical species, ...), so the flux is given by $f = -\beta(x)q_x$ and thus

$$q_t = (\beta(x)q_x)_x. \tag{3.29}$$

It is useful to combine advection and diffusion gives the flux $f = \overline{u}q - \beta q_x$ and results in the *advection-diffusion* equation

$$q_t + \overline{u}q_x = \beta q_{xx}. \tag{3.30}$$

3.4 Heat Equation

Consider the density of internal energy

$$E(x,t) = \kappa(x,t)q(x,t), \tag{3.31}$$

with $\kappa(x,t)$ being the *heat capacity* of the material. The heat flux is then given by *Fourier's law of heat conduction*

$$\text{flux} = -\beta q_x, \tag{3.32}$$

where β is the *coefficient of thermal conductivity*. This looks identical to Fick's law for diffusion, except that Fourier's law states that the *energy* flux is proportional to the temperature gradient. If the heat capacity is identically constant $\kappa \equiv 1$, then this is identical to Fick's law, but there is a fundamental difference if κ varies. More generally

$$\frac{d}{dt}\int_{x_1}^{x_2} \kappa(x)q(x,t)dx = -\beta(x)q_x(x,t)\Big|_{x_1}^{x_2} \tag{3.33}$$

and gives

$$(\kappa q)_t = (\beta q_x)_x. \tag{3.34}$$

Typically κ does not vary with time and thus

$$\kappa q_t = (\beta q_x)_x. \tag{3.35}$$

3.5 Nonlinear Equations in Fluid Dynamics

Usually we are not just interested in the concentration of a tracer in a pipe. The density of the gas also influences the system via the pressure, so the velocity is not a constant but a coupled variable. We therefore need to reformulate the simple equation

$$\rho_t + \overline{u}\rho_x = 0 \tag{3.36}$$

with the more general *continuity equation* (representing the conservation of mass)

$$\rho_t + (\rho u)_x = 0 \tag{3.37}$$

We then also need an evolution equation for the velocity. The velocity itself is not a conserved quantity, but the momentum is with the momentum flux

$$\text{momentum flux} = \rho u^2 + p \tag{3.38}$$

The integral form of this conservation law reads

$$\frac{d}{dt}\int_{x_1}^{x_2} \rho(x,t)u(x,t) = -\left[\rho u^2 + p\right]_{x_1}^{x_2} \tag{3.39}$$

From this integral we see that it is only a difference in pressure at the ends of the domain that actually change the net momentum.

$$(\rho u)_t + (\rho u^2 + p)_x = 0 \tag{3.40}$$

There are now non-linear terms because products of unknowns appear.

Density and pressure are connected via the equation of state and in many ideal cases the following relation can be assumed

$$P'(\rho) > 0 \quad \text{for } \rho > 0 \tag{3.41}$$

This assumption is important for the hyperbolicity of the system. However, this is not true in case of instabilities. The most prominent one is maybe the thermal instability arising from chemical reactions and the resulting cooling. We will have a look at

how this affects the numerical solution and discuss a solution to this later. For now consider this coupled system with the EOS as algebraic closure relation

$$\rho_t + (\rho u)_x = 0 \tag{3.42}$$

$$(\rho u)_t + (\rho u^2 + P(\rho))_x = 0 \tag{3.43}$$

The system can be written in vector notation

$$q_t + f(q)_x = 0 \tag{3.44}$$

with the following components

$$q = \begin{bmatrix} \rho \\ \rho u \end{bmatrix} = \begin{bmatrix} q^1 \\ q^2 \end{bmatrix} \tag{3.45}$$

$$f(q) = \begin{bmatrix} \rho u \\ \rho u^2 + P(\rho) \end{bmatrix} = \begin{bmatrix} q^2 \\ (q^2)^2/q^1 + P(q^1) \end{bmatrix} \tag{3.46}$$

Generally, for m conservation laws we have $q \in \mathbb{R}^m$ and $f : \mathbb{R}^m \to \mathbb{R}^m$

If q is smooth we can rewrite the equation to

$$q_t + f'(q)q_x = 0 \tag{3.47}$$

with the Jacobian matrix $f'(q)$ with entries $\partial f_i/\partial q_j$. This is called the *quasi-linear form* since is resembles the linear system

$$q_t + Aq_x = 0 \tag{3.48}$$

where A is the $m \times m$ matrix. In the linear case the matrix A does not depend on q, in the quasi-linear case it does!

3.6 Linear Acoustics

Let's have a look at the problem of acoustic waves. We will need the evolution of waves later, because thermal pressure is mediated by sound waves. Acoustic waves are small perturbations in a background medium that do not change the background system macroscopically: The magnitudes of the disturbances are small, so powers of the perturbations can be ignored and we can do a linearisation

$$q(x,t) = q_0 + \tilde{q}(x,t) \tag{3.49}$$

with the background state q_0 and the perturbation $\tilde{q}$. We then end up with the linearised equation

$$\tilde{q}_t + f'(q_0)\tilde{q}_x = 0 \tag{3.50}$$

with the constant coefficient matrix

$$A = f'(q_0) = \begin{bmatrix} 0 & 1 \\ -u_0^2 + P'(\rho_0) & 2u_0 \end{bmatrix} \tag{3.51}$$

Note that the state vector $\tilde{q}$ has components $\tilde{\rho}$ and $\widetilde{\rho u}$ representing the perturbations, so $\tilde{p} \approx P'(\rho_0)\tilde{\rho}$ and $\widetilde{\rho u} \approx u_0\tilde{\rho} + \rho_0\tilde{u}$. We then end up with the linear system

$$\begin{bmatrix} p \\ u \end{bmatrix}_t + \begin{bmatrix} u_0 & K_0 \\ 1/\rho_0 & u_0 \end{bmatrix} \begin{bmatrix} p \\ u \end{bmatrix}_x = 0 \tag{3.52}$$

where $K_0 = \rho_0 P'(\rho_0)$ is the *bulk modulus of compressibility*. An important special case is the static one with $u_0 = 0$, so the linearisation about the motionless state

$$A = \begin{bmatrix} 0 & K_0 \\ 1/\rho_0 & 0 \end{bmatrix} \tag{3.53}$$

where the equations reduce to

$$p_t = K_0 u_x = 0 \tag{3.54}$$

$$\rho_0 u_t + p_x = 0 \tag{3.55}$$

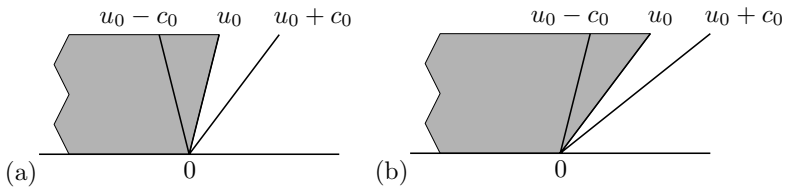

Figure 2: visualisation of the characteristics of the sound waves. The left side shows the subsonic case the right side the supersonic case.

3.7 Sound Waves

Solving this set of equations should give us sound waves moving through the stationary gas. As the equations are linear, we overall expect a superposition of sound waves moving in both directions as a general solution. This suggests to look for solutions of the form

$$q(x,t) = \overline{q}(x - st) \tag{3.56}$$

for some speed s and $\overline{q}$ is some function of one variable. We compute the derivatives

$$q_t(x,t) = -s\overline{q}'(x - st), \quad q_x(x,t) = \overline{q}'(x - st) \tag{3.57}$$

and the equation reduces to

$$A\overline{q}'(x - st) = s\overline{q}'(x - st) \tag{3.58}$$

Here, s is a scalar, while A is a matrix, so s needs to be an eigenvalue of the matrix A and $\overline{q}'$ needs to be the corresponding eigenvector. For the previously found matrix of the acoustic system we find the following eigenvalues

$$\lambda^1 = -c_0 \quad \text{and} \quad \lambda^2 = +c_0 \tag{3.59}$$

with the sound speed

$$c_0 = \sqrt{K_0/\rho_0} = \sqrt{P'(\rho_0)} \tag{3.60}$$

Here, we can directly see numerical problems in case of $P'(\rho_0) < 0$ in thermally unstable regions. In addition there is also a fundamental problem of grid codes for $\rho_0 \to 0$. This means that the density in the cells cannot be zero and sensible minimum values have to be found carefully. For the more general case with non-zero u_0 the eigenvalues read

$$\lambda^1 = u_0 - c_0 \quad \text{and} \quad \lambda^2 = u_0 + c_0. \tag{3.61}$$

The visualisation of the characteristics is shown in figure 2 for subsonic velocities $u_0 < c_0$ (a) and supersonic velocities $u_0 > c_0$ (b).

Regardless of the value of u_0 the eigenvectors are

$$r^1 = \begin{bmatrix} -\rho_0 c_0 \\ 1 \end{bmatrix}, \quad r^2 = \begin{bmatrix} \rho_0 c_0 \\ 1 \end{bmatrix}, \tag{3.62}$$

A sound wave propagating to the left with velocity $-c_0$ must have the general form

$$q(x,t) = \overline{w}^1(x + c_0 t)r^1 \tag{3.63}$$

for some scalar function $\overline{w}^1$, so that

$$q(x,t) = \overline{w}^1(x + c_0 t)r^1 \equiv \overline{q}(x + c_0 t) \tag{3.64}$$

The general solution is the superposition of sound waves going to the left and to the right mus then read

$$q(x,t) = \overline{w}^1(x + c_0 t)r^1 + \overline{w}^2(x - c_0 t)r^2 \tag{3.65}$$

3.8 Hyperbolicity of Linear Systems

A linear system of the form

$$q_t + Aq_x = 0 \tag{3.66}$$

is called hyperbolic if the $m \times m$ matrix A is diagonalisable with real eigenvalues

$$\lambda^1 \leq \lambda^2 \leq ... \leq \lambda^m \tag{3.67}$$

The matrix is diagonalisable if there is a *complete* set of linearly independent eigenvectors $r^1, r^2, ..., r^m \in \mathbb{R}^m$

$$Ar^p = \lambda^p r^p \quad \text{for } p = 1, 2, ...m \tag{3.68}$$

In this case the matrix formed by the eigenvalues

$$R = \left[r^1 | r^2 | ... | r^m\right] \tag{3.69}$$

is non-singular and has an inverse R^{-1}.

$$R^{-1}AR = \Lambda \quad \text{and} \quad A = R\Lambda R^{-1} \tag{3.70}$$

with

$$\Lambda = \begin{bmatrix} \lambda^1 & & & \\ & \lambda^2 & & \\ & & \ddots & \\ & & & \lambda^m \end{bmatrix} = \text{diag}\left(\lambda^1, \lambda^2, ..., \lambda^m\right) \tag{3.71}$$

The important point for us is that we can rewrite the system in the following form

$$R^{-1}q_t + R^{-1}ARR^{-1}q_x = 0 \tag{3.72}$$

and by defining $w(x,t) \equiv R^{-1}q(x,t)$ the equation takes the simple form

$$w_t + \Lambda w_x = 0 \tag{3.73}$$

Since Λ is diagonal, the system decouples into m independent advection equations for the components w^p

$$w_t^p + \lambda^p w_x^p = 0 \quad \text{for } p = 1, 2, ..., m \tag{3.74}$$

All eigenvalues λ^p are real and can thus be used in a physical sense to solve a system of conservation equations. The solutions will consist of a linear combination of m "waves" travelling at speeds λ^p. These values define the *characteristic curves* $X(t) = x_0 + \lambda^p t$ along which information propagates in the decoupled advection equations. The functions $w^p(x,t)$ are called *characteristic variables*.

3.9 Variable-Coefficient Hyperbolic Systems

Let's have a look at the system with variable coefficients

$$q_t + A(x)q_x = 0 \tag{3.75}$$

This system is hyperbolic at any point x where the coefficient matrix satisfies the above mentioned conditions.

In some cases we have a conservative system of linear equations of the form

$$q_t + (A(x)q)_x = 0 \tag{3.76}$$

in which the flux function $f(q,x)$ explicitly depends on x. This system can be rewritten as

$$q_t + A(x)q_x = -A'(x)q, \tag{3.77}$$

so a system of the form (3.75) with an additional *source term*.

4 Characteristics and Riemann Problems for Linear Hyperbolic Equations

Here we further explore the characteristic structure of linear hyperbolic equations. We focus on solutions to the *Riemann problem*, which is simply the given equation together with special initial, piecewise constant data with a single jump condition. The advection equation reads

$$q_t + A(x)q_x = 0 \tag{4.1}$$

and the system is hyperbolic if A is diagonalisable with real eigenvalues

$$A = R\Lambda R^{-1}, \tag{4.2}$$

where R is the matrix of right eigenvectors. Introducing new variables

$$w = R^{-1}q \tag{4.3}$$

allows us to reduce the system to m decoupled advection equations.

$$w_t + \Lambda w_x = 0 \tag{4.4}$$

Note that this assumes that A is constant. If A varies with x and/or t, then the system is still linear but R and Λ will generally also depend on x and t and the simplification to equation (4.4) is not possible!

From this we can compute data

$$\mathring{w}(x) \equiv R^{-1}\mathring{q}(x) \tag{4.5}$$

for the system. The pth equation is given by

$$w^p_t + \lambda^p w^p_x = 0 \tag{4.6}$$

with the solution

$$w^p(x,t) = w^p(x - \lambda^p t, 0) = \mathring{w}^p(x - \lambda^p t) \tag{4.7}$$

Having computed all components we can combine them to obtain

$$q(x,t) = Rw(x,t) \tag{4.8}$$

As the system is linear we write the vector as a linear combination of the right eigenvectors and thus as a superposition of the waves propagating at speeds λ^p

$$q(x,t) = \sum_{p=1}^{m} w^p(x,t)r^p \tag{4.9}$$

The values w^p represent the *strength* of the waves. The eigencoefficient $\mathring{w}^p(x) = w^p(x,0)$ is simply advected at constant speed λ^p as time evolves all along the curve $X(t) = x_0 + \lambda^p t$, the p-characteristics. If the system is strictly hyperbolic, m curves pass through each point in the $x - t$ plane.

4.1 Left Eigenvectors

Define $L = R^{-1}$ and find the left eigenvectors (rows of L)

$$l^p A = \lambda^p l^p \tag{4.10}$$

We can write the characteristic variable $w^p(x,t)$, which is the pth component of the $R^{-1}q(x,t) = Lq(x,t)$, simply as

$$w^p(x,t) = l^p q(x,t) \tag{4.11}$$

We can then write the solution vector in terms of the initial data $\mathring{q}$ and the eigenvectors

$$q(x,t) = \sum_{p=1}^{m} \left[l^p \mathring{q}(x - \lambda^p t)\right] r^p \tag{4.12}$$

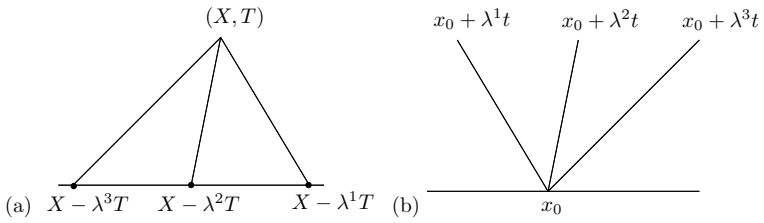

Figure 3: domain of dependence and range of influence for a typical hyperbolic system with three eigenvalues.

4.2 Domain of Dependence and Range of Influence

Let's take some fixed point (X, T) in space-time. We see from equation (4.12) that the solution $q(X, T)$ is entirely given by the initial data propagated along the characteristic curves $X - \lambda^p t$ for $p = 1, 2, ..., m$. From these characteristic curves we can define a set of points

$$\mathcal{D}(X, T) = (X - \lambda^p T : p = 1, 2, ..., m) \tag{4.13}$$

that is called the *domain of dependence*, see also figure 3. The value of the initial data at other points does not have an influence on the data at point (X, T).

For hyperbolic systems with finite eigenvalues, the domain of dependence is always bounded! Contrary, for non-linear equations the solution may depend on the entire domain rather than a subset of points within the domain. This has an important consequence for the design of numerical methods. For systems with finite propagation speeds we can use explicit methods efficiently. For infinite speeds implicit methods need to be used.

We can see that by looking at the heat equation $q_t = -\beta q_{xx}$. The domain of dependence of any point is the entire real line. Changing the data anywhere would in principle change the result anywhere else in the domain. Imagine a delta distribution at time t_0 somewhere in the domain. After some time dt, no matter how small dt is, the diffusion or heat equation will have the functional form of a Gaussian with infinite wings, so infinite propagation speed. This also shows that the pure diffusion equation is only a mathematical equation with unphysical effects in extreme cases.

Another example is the Poisson equation and the resulting gravitational force. "As soon as" you place some additional mass somewhere the changes in the gravitational potential will affect matter everywhere in the domain, provided the changes in the gravitational potential travel infinitely fast.

For these equations (parabolic systems) we generally use implicit methods.

You can also turn around the viewpoint and look at the range of influence of a certain point, see right panel in figure 3.

4.3 Discontinuous Solutions

Classical solutions of differential equations must be smooth. In contrast, given some physical systems and in particular discretised systems can have discontinuities already at the beginning in the initial data or can develop them later during the evolution of the system. Discontinuities in the solution correspond to singularities in the differential equation. If the system has some discontinuity in the initial data $\mathring{q}(x)$ (and a singularity in the differential equation) and the system is propagated in time along the characteristics the singularities and discontinuities can also propagate into the solutions $q(x, t)$,

Conversely, if the data is smooth in the neighbourhood of all points $\overline{x} - \lambda^p \overline{t}$, then the solution $q(x, t)$ must also be smooth in the neighbourhood of the point $(\overline{x}, \overline{t})$. This means that singularities can *only* travel along characteristics of the linear system!

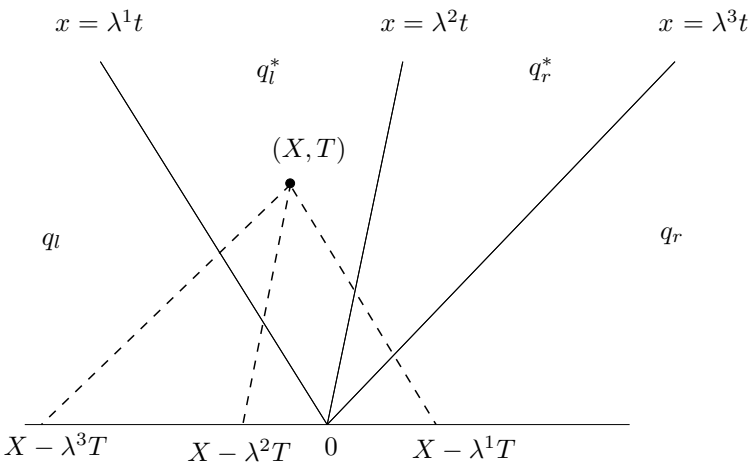

Figure 4:

4.4 Riemann Problem for a Linear System

The *Riemann problem* consists of the hyperbolic equation together with special initial data that is piecewise constant with some jump condition

$$\mathring{q}(x) = \begin{cases} q_l & \text{if } x < 0 \\ q_r & \text{if } x > 0 \end{cases} \tag{4.14}$$

We now expect this jump to propagate along the characteristics. We can decompose the solution into left and right part

$$q_l = \sum_{p=1}^{m} w_l^p r^p \quad \text{and} \quad q_r = \sum_{p=1}^{m} w_r^p r^p \tag{4.15}$$

where the pth advection equation has Riemann data

$$\mathring{w}^p(x) = \begin{cases} w_l & \text{if } x < 0 \\ w_r & \text{if } x > 0 \end{cases} \tag{4.16}$$

and the discontinuity propagates with speed λ^p, so

$$\mathring{w}^p(x,t) = \begin{cases} w_l & \text{if } x - \lambda^p t < 0 \\ w_r & \text{if } x - \lambda^p t > 0 \end{cases} \tag{4.17}$$

Let $P(x,t)$ be the maximum value of p for which $x - \lambda^p t > 0$, then

$$q(x,t) = \sum_{p=1}^{P(x,t)} w_r^p r^p + \sum_{p=P(x,t)+1}^{m} w_l^p r^p \tag{4.18}$$

which can be written in shorter notation

$$q(x,t) = \sum_{p:\lambda^p < x/t} w_r^p r^p + \sum_{p:\lambda^p > x/t} w_l^p r^p \tag{4.19}$$

The determination of the solution at point (X, T) is illustrated in figure 4 for three waves. The solution is constant at any point in the wedges between $x = \lambda^1 t$ and $x = \lambda^2 t$ characteristics. As we cross the pth characteristic, the value of $x - \lambda^p t$ passes through 0 and the corresponding w^p jumps from w_l^p to w_r^p. This jump is an eigenvector of the matrix A, so a scalar multiple of r^p. This jump condition is called *Rankine-Hugoniot jump condition* and will be derived from the integral form of the conservation law. This jump condition also holds across any propagating discontinuity. Typically the data (q_l, q_r) does not satisfy this condition and the process of solving the Riemann problem can be viewed as an attempt to split up the jump $q_r - q_l$ into a series of

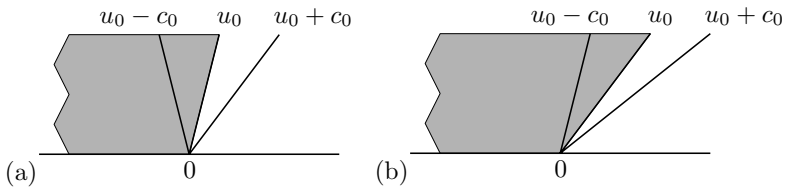

Figure 5: visualisation of the characteristics of the sound waves. The left side shows the subsonic case the right side the supersonic case.

jumps, defined by different individual waves that satisfy the condition. The jump is then decomposed into eigenvectors

$$q_r - q_l = \alpha^1 r^1 + ... + \alpha^m r^m \tag{4.20}$$

By introducing the notation

$$\mathcal{W}^p = \alpha^p r^p \tag{4.21}$$

we can write the solution to the problem in the form

$$q(x,t) = q_l + \sum_{p:\lambda^p < x/t} \mathcal{W}^p \tag{4.22}$$

$$= q_r - \sum_{p:\lambda^p \geq x/t} \mathcal{W}^p \tag{4.23}$$

or

$$q(x,t) = q_l + \sum_{p=1}^{m} H(x - \lambda^p t)\mathcal{W}^p \tag{4.24}$$

where H is the *Heavyside step function.*

4.5 Coupled acoustics and Advection

Consider acoustics in a fluid moving with some speed u_0. In addition consider a tracer that is advected with the flow (see figure 5). Let the fluid on the left (including the tracer) be "black" and on the right (without tracer) be "white". The system can be described by the equation

$$\begin{bmatrix} p \\ u \\ \phi \end{bmatrix}_t + \begin{bmatrix} u_0 & K_0 & 0 \\ 1/\rho_0 & u_0 & 0 \\ 0 & 0 & u_0 \end{bmatrix} \begin{bmatrix} p \\ u \\ \phi \end{bmatrix}_x \tag{4.25}$$

The system has the following eigenvalues

$$\lambda^1 = u_0 - c_0, \quad \lambda^2 = u_0, \quad \lambda^3 = u_0 + c_0, \tag{4.26}$$

The 1-wave and 3-wave are standard acoustic waves independent of ϕ, the 2-wave gives the advection of ϕ. Figure 5 shows the regions. The two fluids remain in contact at the second characteristic curve the dynamics of the system does not have an effect in this regime, so the pressure does not change. This characteristics is called *contact discontinuity.*

Within each of the fluids there is a sound wave moving at speed c_0 (relative to the fluid) away from the origin. The jump in pressure and/or velocity creates a "noise" that moves through the fluid with the speed of sound.

5 Finite Volume Methods

Finite volume methods are closely related to finite difference methods, and a finite volume method can often be interpreted as an approximation to a finite difference method. However, the finite volume method is derived and based on the integral description of the conservation law, which turns out to have some important advantages.

5.1 General Formulation for Conservation Laws

Whereas for a finite difference method the domain is divided into discrete *points*, the finite volume method considers *grid cells* with the central point of the grid cell being the measuring point of the quantities under consideration. In finite volume methods we keep track of the integral over this grid cell and update the value in the cells according to the fluxes at the boundaries of the grid cells. The value in the cell is given by the average of the integral function

$$Q_i^n = \frac{1}{\Delta x} \int_{x_{i-1/2}}^{x_{i+1/2}} q(x, t_n) dx \tag{5.1}$$

Δx is the length of the cell. If $q(x,t)$ is a smooth function, the integral equals the value at the midpoint of the interval to order $\mathcal{O}(\Delta x^2)$. Numerically the sum over the cells $\sum_i Q_i^n \Delta x$ approximates the integral of q over the domain. Integrating the integral form of the conservation law

$$\frac{d}{dt} \int_{x_{i-1/2}}^{x_{i+1/2}} q(x,t) dx = f\left(q\left(x_{i-1/2}, t\right)\right) - f\left(q\left(x_{i+1/2}, t\right)\right) \tag{5.2}$$

in time about $\Delta t = t_{n+1} - t_n$ and rearranging the equation gives

$$\begin{aligned} &\frac{1}{\Delta x} \int_{x_{i-1/2}}^{x_{i+1/2}} q(x, t_{n+1}) dx = \frac{1}{\Delta x} \int_{x_{i-1/2}}^{x_{i+1/2}} q(x, t_n) dx \\ &- \frac{1}{\Delta x} \left[\int_{t_n}^{t_{n+1}} f\left(q\left(x_{i+1/2}, t\right)\right) dt - \int_{t_n}^{t_{n+1}} f\left(q\left(x_{i-1/2}, t\right)\right) dt \right] \end{aligned} \tag{5.3}$$

This tells us exactly how the cell average of q should be updated in one time step. We have to study numerical methods of the form

$$Q_i^{n+1} = Q_i^n - \frac{\Delta t}{\Delta x} \left(F_{i+1/2}^n - F_{i-1/2}^n \right) \tag{5.4}$$

where $F_{i-1/2}^n$ is some approximation to the fluxes between the cell boundary at $x = x_{i-1/2}$.

$$F_{i-1/2} \approx \frac{1}{\Delta t} \int_{t_n}^{t_{n+1}} f\left(q\left(x_{i-1/2}, t\right)\right) dt \tag{5.5}$$

This flux should be computed using the cell centered values Q_i using a *numerical flux* $\mathcal{F}$

$$F_{i-1/2}^n = \mathcal{F}\left(Q_{i-1}^n, Q_i^n\right) \tag{5.6}$$

The design of the numerical flux can differ but the easiest methods will be an explicit method with a *three-point stencil*, meaning that the value Q_i^{n+1} will depend on Q_{i-1}^n, Q_i^n, and Q_{i+1}^n at the previous time level. Derived from a conservative form, the following sum holds for any subset of the domain.

$$\Delta x \sum_{i=I}^{J} Q_i^{n+1} = \Delta x \sum_{i=I}^{J} Q_i^n - \frac{\Delta t}{\Delta x} \left(F_{J+1/2}^n - F_{I-1/2}^n \right) \tag{5.7}$$

The sum of the flux differences between the individual cells cancels out by construction of the method except for the fluxes at the extreme edges. Rearranging gives

$$\frac{Q_i^{n+1} - Q_i^n}{\Delta t} + \frac{F_{i+1/2}^n - F_{i-1/2}^n}{\Delta x} = 0 \tag{5.8}$$

5.2 Numerical Flux for the Diffusion Equation

Let's now consider an example where the flux depends on x, the diffusion equation, where the flux is

$$f(q_x, x) = -\beta(x) q_x \tag{5.9}$$

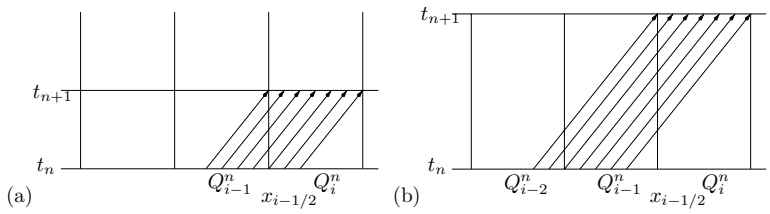

Figure 6: visualisation of the CFL condition for an appropriate time step (left) and a time step that is too large for the characteristics (right).

Given two cell averages Q_{i-1} and Q_i, the numerical flux can be defined as

$$\mathcal{F}(Q_{i-1}, Q_i) = -\beta_{i-1/2}\left(\frac{Q_i - Q_{i-1}}{\Delta x}\right) \tag{5.10}$$

where we take $\beta_{i-1/2} \approx \beta(x_{i-1/2})$. The standard difference discretisation gives

$$Q_i^{n+1} = Q_i^n + \frac{\Delta t}{\Delta x^2}\left[\beta_{i+1/2}\left(Q^n_{i+1} - Q^n_i\right) - \beta_{i-1/2}\left(Q^n_i - Q^n_{i-1}\right)\right] \tag{5.11}$$

If β is constant everywhere then

$$Q_i^{n+1} = Q_i^n + \frac{\Delta t}{\Delta x^2}\beta\left[Q^n_{i-1} - 2Q^n_i + Q^n_{i+1}\right] \tag{5.12}$$

Parabolic equations are usually solved using implicit methods because the explicit method requires time steps $\Delta t \propto \Delta x^2$, whereas the implicit method is unconditionally stable for all time steps. With the *Crank-Nicolson method* the new states are computed with

$$\begin{aligned} Q_i^{n+1} = Q_i^n + \frac{\Delta t}{\Delta x^2}\big[&\beta_{i+1/2}\left(Q^n_{i+1} - Q^n_i\right) - \beta_{i-1/2}\left(Q^n_i - Q^n_{i-1}\right) \\ &+\beta_{i+1/2}\left(Q^{n+1}_{i+1} - Q^{n+1}_i\right) - \beta_{i-1/2}\left(Q^{n+1}_i - Q^{n+1}_{i-1}\right)\big] \end{aligned} \tag{5.13}$$

which can be viewed as finite volume method with the flux

$$F^n_{i-1/2} = -\frac{1}{2\Delta x}\left[\beta_{i-1/2}\left(Q^n_i - Q^n_{i-1}\right) + \beta_{i-1/2}\left(Q^{n+1}_i - Q^{n+1}_{i-1}\right)\right] \tag{5.14}$$

This is a natural approximation to the time averaged flux and is in fact second-order accurate in both space and time.

Note on implicit methods Implicit methods are unconditionally stable for all time steps, which can be essential for solving systems. A set of stiff ODEs can have time steps that insanely small. Without implicit methods, these systems cannot be solved. However, the stability of implicit systems does not include the convergence to the correct solution! For implicit methods the information of the new time step needs to be included. This means that you have to solve a matrix equation. In multidimensional systems this matrix is generally too big to solve!

5.3 The CFL condition

The CFL condition (after Courant, Friedrichs, and Lewy, (1928)) is a necessary although not sufficient criterion for numerical convergence of an explicit scheme. It simply states that the information that travels through the domain has a chance to propagate appropriately. The explicit method with a three-point stencil uses Q^n_{i-1}, Q^n_i, and Q^n_{i+1} to compute the state Q^{n+1}_i. As the solution "travels" along the characteristics of the system, we need to make sure that the time integration step from t_n to t_{n+1} is small enough that the information starting from the centre of the cell does not travel further than the one cell. See figure 6 for an illustration. On the left we see the situation where $\overline{u}\Delta t < \Delta x$, so information does not travel further than one grid cell. In this case it makes sense to define the flux at $x_{i-1/2}$ only by the terms of Q^n_{i-1} and Q^n_i. On the right, the characteristics travel further than one cell the flux

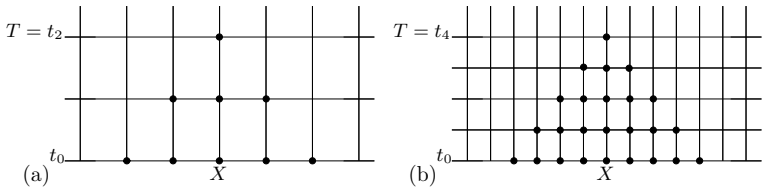

Figure 7: visualisation of the CFL condition and the necessary domain of dependence. Larger time steps or smaller grid cells require more grid points to be included in order to compute the new solution.

at the same boundary is now influenced also by the averaged value Q^n_{i-2}, so for the three-point stencil the time step is too large.

CFL condition: *A numerical method can be convergent only if its numerical domain of dependence contains the true domain of dependence of the PDE, at least in the limit as Δt and Δx go to zero.*

The domain of dependence can be defined in a similar manner as the points that can possibly affect the solution Q^{n+1}_i, see figure 7. The CFL condition requires for the domain of dependence

$$X - T/r \leq X - \overline{u}T \leq X + T/r \tag{5.15}$$

and thus

$$\nu \equiv \left| \frac{\overline{u}\Delta t}{\Delta x} \right| \leq 1 \tag{5.16}$$

If this condition is not satisfied, the initial data *would* change the true solution but *cannot* affect the solution. The method then cannot converge. In systems with many waves, the fastest wave is the dominant limiting wave for the stability criterion,

$$\nu = \frac{\Delta t}{\Delta x} \max_p |\lambda^p|. \tag{5.17}$$

5.4 An Unstable Flux

Before we can actually solve a PDE we need to specify how we compute the numerical fluxes. A first simple attempt to compute the fluxes at the cell boundaries might be the arithmetic average

$$F^n_{i-1/2} = \mathcal{F}(Q^n_{i-1}, Q^n_i) = \frac{1}{2}\left[f(Q^n_{i-1}) + f(Q^n_i)\right] \tag{5.18}$$

which gives the following description for computing the new state

$$Q^{n+1}_i = Q^n_i - \frac{\Delta t}{2\Delta x}\left[f(Q^n_{i+1}) + f(Q^n_{i-1})\right]. \tag{5.19}$$

Unfortunately this flux is unconditionally unstable independent of the CFL number for hyperbolic methods and cannot be used. Later we see, however, that correction terms might solve the stability problem.

5.5 Lax-Friedrichs Method

Without further motivation we show how the classical Lax-Friedrichs scheme looks like:

$$Q^{n+1}_i = \frac{1}{2}\left(Q^n_{i-1} + Q^n_{i+1}\right) - \frac{\Delta t}{2\Delta x}\left[f(Q^n_{i+1}) + f(Q^n_{i-1})\right] \tag{5.20}$$

This is very similar to the unstable method in equation (5.18) but the value Q^n_i is replaced by the average $\frac{1}{2}\left(Q^n_{i-1} + Q^n_{i+1}\right)$. This method is stable. At first sight this method does not look like the general form (equation (5.4)), but with the numerical flux defined as

$$\mathcal{F}(Q^n_{i-1}, Q^n_i) = \frac{1}{2}\left[f(Q^n_{i-1}) + f(Q^n_i)\right] - \frac{\Delta x}{2\Delta t}\left(Q^n_i - Q^n_{i-1}\right) \tag{5.21}$$

we can transform the method in the standard form. We can understand why this method is stable. The numerical flux is basically the unstable flux with the addition of a term that is similar to the flux of the diffusion equation (5.10). By using this flux we appear to model the advection-diffusion equation $q_t + f(q)_x = \beta q_{xx}$ with $\beta = \frac{1}{2}(\Delta x)^2/\Delta t$. But if we fix $\Delta t/\Delta x$ we see that this coefficient vanishes as the grid is refined, so in the limit it is still consistent with the hyperbolic equation. This additional term can be understood as *numerical diffusion* that damps the instabilities that arise in the simple unstable algorithm (5.18). This method can be shown to be stable up to a Courant number of unity.

5.6 The Richtmyer Two-Step Lax-Wendroff Method

The Lax-Wendroff method is only first-order accurate. One can obtain second-order accuracy by a better approximation of the flux integral (5.5), for example by first interpolating the q at the midpoint in time $t_{n+1/2} = t_n + \Delta t/2$ and evaluating the flux at this point. The Richtmyer method uses

$$F^n_{i-1/2} = f(Q^{n+1/2}_{i-1/2}), \tag{5.22}$$

where

$$Q^{n+1/2}_{i-1/2} = \frac{1}{2}\left(Q^n_{i-1} + Q^n_i\right) - \frac{\Delta t}{2\Delta x}\left[f(Q^n_i) + f(Q^n_{i-1})\right]. \tag{5.23}$$

5.7 Upwind Methods

All previous methods are constructed in a symmetric way, i.e., centered about the point where we update the solution. However, in hyperbolic systems the solutions follow the characteristics, which are oriented in specific directions, depending on the eigenvalues. So it is useful to take the additional information into account when constructing a method for the solutions. This leads to *upwind* methods in which the information for each characteristic variable is obtained by looking in the direction from which the information is coming. For the constant-coefficient advection equation $q_t + \overline{u} q_x = 0$ the flux is given by the value of Q^n_{i-1}. This suggests the flux to be defined as

$$F^n_{i-1/2} = \overline{u} Q^n_{i-1}, \tag{5.24}$$

which gives the *first-order upwind method*

$$Q^{n+1}_i = Q^n_i - \frac{\overline{u}\Delta t}{\Delta x}\left(Q^n_i - Q^n_{i-1}\right). \tag{5.25}$$

We can also interpret the evolution of Q^n_i as being the translated information along the characteristics

$$Q^{n+1}_i \approx q(x_i, t_{n+1}) = q(x_i - \overline{u}\Delta t, t_n). \tag{5.26}$$

Interpolating between the grid points Q^n_{i-1} and Q^n_1 gives

$$Q^{n+1}_i = \frac{\overline{u}\Delta t}{\Delta x} Q^n_{i-1} + \left(1 + \frac{\overline{u}\Delta t}{\Delta x}\right) Q^n_i, \tag{5.27}$$

which is exactly the upwind method after rearranging the equation. If the velocity is negative, then the flux should be defined

$$F^n_{i-1/2} = \overline{u} Q^n_i \tag{5.28}$$

and the upwind method has the form

$$Q^{n+1}_i = Q^n_i - \frac{\overline{u}\Delta t}{\Delta x}\left(Q^n_{i+1} - Q^n_i\right). \tag{5.29}$$

The two formulas can be combined into a single equation

$$F^n_{i-1/2} = \overline{u}^- Q^n_i + \overline{u}^+ Q^n_{i-1}, \tag{5.30}$$

where the velocities are extended with "switches"

$$\overline{u}^+ = \max(\overline{u}, 0), \qquad \overline{u}^- = \min(\overline{u}, 0). \tag{5.31}$$

5.8 Godunov method

- upwind, finite volume method for hyperbolic system in the context of constant-coefficient linear systems
- first order accurate
- introduces a lot of numerical diffusion, poor accuracy, smeared-out results

$$Q_i^{n+1} = Q_i^n - \frac{\Delta t}{\Delta x}\left[\sum_{p=1}^{m}(\lambda^p)^+\mathcal{W}_{i-1/2}^p + \sum_{p=1}^{m}(\lambda^p)^-\mathcal{W}_{i+1/2}^p\right] \tag{5.32}$$

Introduce a shorthand notation in order to simplify subsequent improvements.

$$\mathcal{A}^-\Delta Q_{i-1/2} = \sum_{p=1}^{m}(\lambda^p)^-\mathcal{W}_{i-1/2}^p \tag{5.33}$$

$$\mathcal{A}^+\Delta Q_{i-1/2} = \sum_{p=1}^{m}(\lambda^p)^+\mathcal{W}_{i-1/2}^p \tag{5.34}$$

This gives a simple equation for the computation of the Godunov scheme

$$Q_i^{n+1} = Q_i^n - \frac{\Delta t}{\Delta x}\left(\mathcal{A}^+\Delta Q_{i-1/2} + \mathcal{A}^-\Delta Q_{i+1/2}\right) \tag{5.35}$$

6 High Resolution Methods

Start with the Godunov scheme. Disadvantage: Introduces a lot of numerical diffusion, poor accuracy, smeared-out results, only first order accurate. This method can be greatly improved by introducing correction terms into equation (5.35)

$$Q_i^{n+1} = Q_i^n - \frac{\Delta t}{\Delta x}\left(\mathcal{A}^+\Delta Q_{i-1/2} + \mathcal{A}^-\Delta Q_{i+1/2}\right) - \frac{\Delta t}{\Delta x}\left(\tilde{F}_{i+1/2} - \tilde{F}_{i-1/2}\right) \tag{6.1}$$

The fluxes $\tilde{F}_{i-1/2}$ are based on the waves resulting from the Riemann solution, which have been computed for the term $\mathcal{A}^\pm\Delta Q_{i-1/2}$. The goal is to combine the Lax-Wendroff approach with a flux limiter.

6.1 Lax-Wendroff Method

The Lax-Wendroff method for the linear system $q_t + Aq_x = 0$ is based on the Taylor expansion

$$q(x, t_{n+1}) = q(x, t_n) + \Delta t q_t(x, t_n) + \frac{1}{2}(\Delta t)^2 q_{tt}(x, t_n) + ... \tag{6.2}$$

From the differential equation we can replace the temporal derivatives with the spatial equivalent giving

$$q_{tt} = -Aq_{xt} = A^2 q_{xx} \tag{6.3}$$

where $q_{xt} = q_{tx} = (-Aq_x)_x$. Keeping only the first three terms and replacing the spatial derivatives by central finite difference approximations gives the *Lax-Wendroff method.*

$$Q_i^{n+1} = Q_i^n - \frac{\Delta t}{2\Delta x}A\left(Q_{i+1}^n + Q_{i-1}^n\right) + \frac{1}{2}\left(\frac{\Delta t}{\Delta x}\right)^2 A^2\left(Q_{i+1}^n + 2Q_i^n + Q_{i-1}^n\right) \tag{6.4}$$

By matching these terms in the Taylor series and using the centered approximation we end up with a second-order accurate method. This algorithm is equivalent to a finite volume method with the following flux

$$F_{i-1/2}^n = \frac{1}{2}A\left(Q_{i-1}^n + Q_i^n\right) - \frac{1}{2}\frac{\Delta t}{\Delta x}A^2\left(Q_i^n - Q_{i-1}^n\right) \tag{6.5}$$

This looks again like the unstable flux in equation (5.18) plus a diffusive flux. Note that the diffusion term exactly matches the what appears in the Taylor expansion.

By matching the first three terms in the series expansion, the dominant error is given by the therm $q_{ttt} = -A^3 q_{xxx}$. This is a *dispersive* term, which leads to oscillations, in particular near discontinuities, but not only there. Even smooth solutions might cause oscillations. The symmetric approach with a centered three-point method is a good candidate for introducing these oscillations.

7 Limiters

In order to solve the problem with oscillations, it seems desirable to use upwind methods that keep the solutions monotonically varying where they should be monotone. However, the accuracy of the upwind method is not very good. The idea is therefore to combine the best features of stable (but less accurate) and sensitive (but accurate) methods. We would like to use second-order accuracy where possible but do not insist on it where the solution does not behave smoothly. This can be achieved using limiters, which gives (without a derivation)

$$F^n_{i-1/2} = \mathcal{F}_L(Q_{i-1}, Q_i) + \phi^n_{i-1/2} \left[\mathcal{F}_H(Q_{i-1}, Q_i) - \mathcal{F}_L(Q_{i-1}, Q_i)\right]. \tag{7.1}$$

If $\phi^n_{i-1/2} = 0$ the flux reduces to a low-order method, if $\phi^n_{i-1/2} = 1$ the high-order method is used.

Defining the "detection" quantity θ

$$\theta^n_{i-1/2} = \frac{\Delta Q^n_{I-1/2}}{\Delta Q^n_{i-1/2}} = \frac{Q^n_I - Q^n_{I-1}}{Q^n_i - Q^n_{i-1}}, \tag{7.2}$$

where the index I is used to represent the interface on the upwind side

$$I = \begin{cases} i-1 & \text{if } \overline{u} > 0 \\ i+1 & \text{if } \overline{u} < 0. \end{cases} \tag{7.3}$$

The ratio $\theta^n_{i-1/2}$ can be thought of as a measure of the smoothness of the data. Here is a list of common limiters

Linear methods:

$$\text{upwind: } \phi(\theta) = 0, \tag{7.4}$$
$$\text{Lax-Wendroff: } \phi(\theta) = 1, \tag{7.5}$$
$$\text{Beam Warming: } \phi(\theta) = \theta, \tag{7.6}$$
$$\text{Fromm: } \phi(\theta) = \frac{1}{2}(1+\theta) \tag{7.7}$$

High-resolution methods:

$$\text{minmod: } \phi(\theta) = \text{minmod}(1, \theta), \tag{7.8}$$
$$\text{superbee: } \phi(\theta) = \max(0, \min(1, 2\theta), \min(2, \theta)), \tag{7.9}$$
$$\text{MC: } \phi(\theta) = \max(0, \min((1+\theta)/2, 2, 2\theta)), \tag{7.10}$$
$$\text{van Leer: } \phi(\theta) = \frac{\theta + |\theta|}{1 + |\theta|}. \tag{7.11}$$

8 Source terms

So far we considered only homogeneous conservation laws of the form $q_t + f(q)_x = 0$. We now have a look at inhomogeneous equations with source terms

$$q_t + f(q)_x = \psi(q). \tag{8.1}$$

Examples for source terms are

- reacting flows

- (self-)gravity modified momentum equation

$$(\rho u)_t + (\rho u^2 + p)_x = -g\rho \tag{8.2}$$

- geometric source terms
- higher order derivatives

8.1 Fractional-Step Method

We have look at the case where the homogeneous system

$$q_t + f(q)_x = 0 \tag{8.3}$$

is hyperbolic and the source terms only depend on the state q and or the position x but not on derivatives of q. In this case the equation

$$q_t = \psi(q) \tag{8.4}$$

reduces to an independent system of ordinary differential equations at each point x. The standard approach to solve this equation is the *fractional-step method* or *operator splitting*, in which we alternate between solving the simpler problems (8.3) and (8.4) to solve the full problem (8.1).

9 Multidimensional Flows

Let us expand the problems before into three dimensions. The conservation law then takes the form

$$q_t + f(q)_x + g(q)_y + h(q)_z = 0. \tag{9.1}$$

Now $q(x, y, z, t)$ depends on all three spatial coordinates. In quasi-linear notation the individual coefficients might depend on all three variables

$$q_t + A(x, y, z, t)q_x + B(x, y, z, t)q_y + C(x, y, z, t)q_z + 0. \tag{9.2}$$

In the derivation of the conservation laws we now need to integrate over the 3D volume and consider the fluxes through the surface of the 3D volume. To check the hyperbolicity of the system we need to investigate a linear combination for all three dimensions

$$\overrightarrow{n} \cdot \overrightarrow{A} = n^x A + n^y B + n^z C \tag{9.3}$$

where $\overrightarrow{n}$ is the orientation vector. In the advection problem with three speeds $(\overline{u}, \overline{v}, \overline{w})$ the solution simply extends to

$$q_(x, y, z, t) = \mathring{q}(x - \overline{u}t, y - \overline{v}t, z - \overline{w}t) \tag{9.4}$$

You can carry the additional dimensions along in all the previous analysis and end up with the three-dimensional Euler equations

$$q = \begin{bmatrix} \rho \\ \rho u \\ \rho v \\ \rho w \\ E \end{bmatrix}, f(q) = \begin{bmatrix} \rho u \\ \rho u^2 + p \\ \rho uv \\ \rho uw \\ (E + p)u \end{bmatrix}, g(q) = \begin{bmatrix} \rho v \\ \rho uv \\ \rho v^2 + p \\ \rho vw \\ (E + p)v \end{bmatrix}, h(q) = \begin{bmatrix} \rho w \\ \rho uw \\ \rho vw \\ \rho w^2 + p \\ (E + p)w \end{bmatrix} \tag{9.5}$$

10 Multidimensional Numerical Methods

10.1 Split Methods

The easiest way of extending the computation in one dimension to two or three dimensions is done via *dimensional splitting*. This in application of the previously discussed fractional-step procedure. The multidimensional problem is split into a

sequence of one-dimensional problems. In a Cartesian grid this is easy to apply. The equation

$$q_t = Aq_x + Bq_y + Cq_z = 0 \tag{10.1}$$

will be split into *sweeps*

$$x - \text{sweep: } q_t + Aq_x = 0 \tag{10.2}$$
$$y - \text{sweep: } q_t + Bq_y = 0 \tag{10.3}$$
$$z - \text{sweep: } q_t + Cq_z = 0 \tag{10.4}$$

We subsequently compute fluxes in each direction and update the cell average. We start with Q^n_{ijk} at time t_n and update it to Q^*_{ijk} along x, keeping the variables j, k for y, z constant

$$Q^*_{ijk} = Q^n_{ijk} - \frac{\Delta t}{\Delta x}\left(F^n_{i+1/2,j,k} - F^n_{i-1/2,j,k}\right) \tag{10.5}$$

where $F^n_{i+1/2,j,k}$ is the appropriate flux for the one-dimensional problem. Analogously we continue

$$Q^{**}_{ijk} = Q^*_{ijk} - \frac{\Delta t}{\Delta x}\left(G^*_{i,j+1/2,k} - G^*_{i,j-1/2,k}\right) \tag{10.6}$$

and compute the final state with

$$Q^{n+1}_{ijk} = Q^{**}_{ijk} - \frac{\Delta t}{\Delta x}\left(H^{**}_{i,j,k+1/2} - H^{**}_{i,j,k-1/2}\right). \tag{10.7}$$

Note that there will be a splitting error unless the operators $\mathcal{A} = A\partial_x$, $\mathcal{B} = B\partial_y$, and $\mathcal{C} = C\partial_z$ commute, i.e., $ABC = CBA$. Only where the multi-dimensional problem decouples into scalar equations we can use dimensional splitting without introducing a splitting error.

In practical cases the splitting error is often not worse than the error you introduce using the one-dimensional integration. Therefore, splitting is a very efficient approach and is widely used. One big advantage is that you can "reuse" the memory, which keeps the memory consumption small compared to unsplit methods, where all intermediate states, interpolations etc. need to be stored simultaneously for all three dimensions.

With this splitting approach we do not explicitly model cross-derivatives involving q_{xy}. In each sweep we only compute derivatives in one direction q_{xx}, q_{yy}. The q_{xy} term arises automatically through the fractional-step procedure. The intermediate states Q^* resulting from the x-sweep models the term Aq_x. Applying the y-sweep afterwards models Bq^*_y and thus models $B(Aq_x)_y$.

There are also other methods of splitting the computation, see, e.g., *strang splitting*, where the sweeps are not done with the same time interval

$$Q^* = x\text{-sweep}(\Delta t/2) \tag{10.8}$$
$$Q^{**} = y\text{-sweep}(\Delta t) \tag{10.9}$$
$$Q^{n+1} = x\text{-sweep}(\Delta t/2) \tag{10.10}$$

10.2 Unsplit Methods

Contrary to the split methods there are also methods that solve the multidimensional problem in one step without using the fractional splitting. These methods are generally more difficult and more memory consuming. In astrophysics they are used much less than the split methods and I don't want to discuss them here. However, as the unsplit method computes all derivatives at the same time they are better for computing magnetic fields.

11 Resolution Limits

Mathematically, the resolution limit is easy to define, it is one cell. Physically, the resolution limit can be significantly larger because certain quantities are not properly captured at the scale of one cell. In SPH the smoothing over N neighbouring

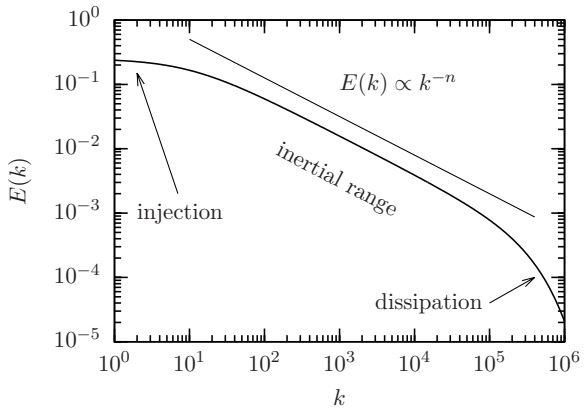

Figure 8: Schematic plot of the turbulent spectrum

particles is a basic assumption that ensures that all physical quantities are statistically "representative" quantities. In grid codes it strongly depends on the quantity you are interested in. For gravitationally bound objects, a resolution of at least 4 cells is needed to follow the collapsing object properly. In turbulence simulations the compressive and solenoidal motions are represented differently. Whereas compressive motions can be successfully modelled with a few cells, solenoidal motions need of the order of 30 cells to properly represent rotational motions. Standard solvers therefore overrate the compressive motions on small scales.

12 Adaptive-Mesh Refinement

12.1 General Idea

- so far, we considered only a fixed grid, in the simplest case even uniform
- grids do not follow a natural refinement like N-body systems or SPH ensembles
- refinement needs to be done by hand
  - disadvantage: organisationally complicated, occurs in steps instead of continuously like in SPH, changes the phase space (smaller cell sizes: smaller structures can be resolved, smaller turbulent modes can be captured, more total energy), convergence is not given / not guaranteed
  - advantage: refinement criteria a completely free (pressure, energy, density, ...), local (spatial) refinement, ...

12.2 Energy in AMR-grids

- example turbulent motions
- energy generally injected at large scales (injection scale), see figure 8
- energy cascades from large eddies to smaller eddies (inertial range)
- energy dissipates on small scales (dissipation), in nature, this is usually molecular dissipation, in numerical simulations this is mostly numerical dissipation
- depending on type of turbulence (Kolmogorov, Burgers) the inertial range has a power spectrum following $k^{-5/3}$, k^{-2}
- The total energy in the grid is given by the integral

$$E = \int_{k_{\min}}^{k_{\max}} P(k) dk \tag{12.1}$$

- $k_{\max}$ is given by the grid resolution. For higher resolution the simulation contains more small scale turbulent energy. Apart from the fact that the total energy changes between one refinement or derefinement step, there is the problem of coupling the effects of the motions at the smallest scales to the grid. As the dissipation at the smallest scales is not physical bu numerical, the turbulent dynamics including the spectrum depends on the spatial resolution. One way out is a subgrid model of turbulence that is coupled to the cells, such that the "true" dissipation scale is shifted to higher k modes and the dynamics in the grid can follow a "proper" inertial range down to the resolution limit.

13 Self-gravitating Systems

- special problem of unstable self-gravitating systems
- Jeans length / Jeans mass

$$\lambda_{\rm J} = \frac{c_{\rm s}}{(G\rho)^{1/2}} \tag{13.1}$$

- consequence fragmenting systems due to self-gravity
- special resolution requirement: Jeans length needs to be resolved with at least 4 cells (Truelove et al. 1997). Otherwise the solver generates artificial fragments, too many fragments.
- this gives a maximum density that the solver and the grid can handle properly

$$\rho_{\max} = \frac{c_{\rm s}^2}{G(4\Delta x)^2} \tag{13.2}$$

- if the density in a cell exceeds this maximum, generate a control volume around this cell, $V = 4\pi/3\,(2\Delta x)^3 = 4\pi/3\,(r_{\rm sink})^3$, and check for certain criteria (see below). If all criteria are fulfilled, then create a Lagrangean sink particle to *hide* mass in order to avoid artificial fragmentation or further refinement.
- sink particles formation criteria
  - grid is at highest refinement
  - local density exceeds threshold density
  - local density is local maximum (local minimum in the graviational potential)
  - the control volume is Jeans unstable (not just a local overdensity in colliding flows)
  - the particle is not in the immediate vicinity of an already existing particle
- various ways of putting mass into the particle
  - put all the mass of the control volume in the sink particle (worst option). Creates a hole in the grid, which leads to artificial external pressure effects.
  - put the excess mass ($M_{\rm exc} = \sum_{\rm cells} \rho_i v_i - \sum_{\rm cells} \rho_{\max} v_i$) into the sink particle
  - take into account the local angular momentum of the gas and *mark* the mass for later accretion
  - sink particle can accrete mass and drive feedback (outflows, radiation, winds, ...)

14 Magneto-Hydrodynamics

14.1 General aspects

Often we need to study flows of (partially) ionised gas in the presence of magnetic fields. The field then exerts a force on the gas and changes the momentum of the gas particles, which in turn perturbs the magnetic field. We thus need to couple the equations for the magnetic field with the Euler (gas) equations. In most cases this is done using a simplified version of Maxwell's equations. The simplifications are chosen because we are interested in the (relatively slow) effect of and on the particle motions and not in the propagation of electromagnetic waves.

For a non-relativistic flow and variations on large time scales we can ignore the displacement current and approximate

$$\mathbf{j} = \frac{1}{4\pi}\nabla \times \mathbf{B} \tag{14.1}$$

$$\mathbf{E} = \mathbf{j}/\sigma - \mathbf{u} \times \mathbf{B} \tag{14.2}$$

and hence

$$\frac{\partial \mathbf{B}}{\partial t} = -\nabla \times \mathbf{E} \tag{14.3}$$

$$\approx \nabla \times (\mathbf{u} \times \mathbf{B}) + \eta \nabla^2 \mathbf{B} \tag{14.4}$$

We have omitted the explicit dependence on the electric field and end up with an evolution equation for the magnetic field that only depends on $\mathbf{B}$ and the gas velocity $\mathbf{u}$. In the case of *ideal MHD* we also neglect the resistivity η so that the dissipative term vanishes.

An additional general condition is the vanishing divergence

$$\nabla \cdot \mathbf{B} = 0. \tag{14.5}$$

Solutions to the MHD equations will automatically maintain (14.5) provided the initial condition fulfilled the condition. Numerically this is not necessarily the case.

The evolution equation for ideal MHD then reads

$$\frac{\partial \mathbf{B}}{\partial t} + \nabla \times (\mathbf{uB} - \mathbf{Bu}) = 0. \tag{14.6}$$

Additional coupling besides the velocity itself is mediated by the force that the magnetic field exerts on the gas, which appears in the momentum equation. The full momentum equation then reads

$$(\rho \mathbf{u})_t + \nabla \left(\rho \mathbf{uu} + I \left(p + \frac{1}{8\pi} B^2 \right) - \frac{1}{4\pi} \mathbf{BB} \right). \tag{14.7}$$

The total energy extends to

$$E = e + \frac{1}{2}\rho u^2 + \frac{1}{8\pi} B^2. \tag{14.8}$$

The overall state and flux in x-direction then look

$$q = \begin{bmatrix} \rho \\ \rho u \\ \rho v \\ \rho w \\ B_x \\ B_y \\ B_z \\ E \end{bmatrix}, f(q) = \begin{bmatrix} \rho u \\ \rho u^2 + p + \frac{1}{2}B^2 - B_x^2 \\ \rho uv - B_x B_y \\ \rho uw - B_x B_z \\ 0 \\ B_y u - v B_x \\ B_z u - w B_x \\ u(E + p + \frac{1}{2}B^2) - B_x(uB_x + vB_y + wB_z) \end{bmatrix} \tag{14.9}$$

Note that here B_x etc. are the directional components and *not* the derivatives!

14.2 One-dimensional MHD

If we only consider the one-dimensional case we immediately see that the flux component for B_x is zero, so

$$\frac{\partial}{\partial t} B_x = 0. \tag{14.10}$$

The equation

$$q_t + f(q)_x = 0 \tag{14.11}$$

reduces to the state

$$\tilde{q} = (\rho, \rho u, \rho v, \rho w, B_y, B_z, E). \tag{14.12}$$

After linearisation of the equations we can determine the characteristic waves and compute the eigenvalues of the Jacobian matrix, giving

$$\lambda^1 = u - c_\mathrm{f} \tag{14.13a}$$
$$\lambda^2 = u - c_\mathrm{A} \tag{14.13b}$$
$$\lambda^3 = u - c_\mathrm{s} \tag{14.13c}$$
$$\lambda^4 = u \tag{14.13d}$$
$$\lambda^5 = u + c_\mathrm{s} \tag{14.13e}$$
$$\lambda^6 = u + c_\mathrm{A} \tag{14.13f}$$
$$\lambda^7 = u + c_\mathrm{f}. \tag{14.13g}$$

Waves are propagating with 3 different speeds relative to the gas ($c_\mathrm{f}, c_\mathrm{A}, c_\mathrm{s}$), see figure 9. The velocity $\lambda^4 = u$ corresponds to the contact discontinuity. Without magnetic fields this continuity can carry arbitrary variation in the transverse velocities v and w as well as in ρ. The shear velocity is simply advected and is not taken into account for gas (ideal fluid, no resistence to shear motion). In MHD this is not valid any more. Ideal MHD couples the magnetic field to the gas ("field lines are frozen in the gas", **B** is transported with the gas), so shear motions will lead to distortion of the field lines and impose a force on the gas. There we have to distinguish between two different waves: compressional waves (called pressure waves or P-waves) that are acoustic waves and transversal waves (shear waves, S-waves) that arise from the transverse displacement and the restoring force. These two kind of waves travel with different speeds ($v_p > v_s$).

Purely transverse waves are known as *Alfvén waves* with speed

$$c_\mathrm{A} = \sqrt{\frac{B_x^2}{4\pi\rho}}, \tag{14.14}$$

which are the 2-wave and the 6-wave. Like the contact discontinuity, the Alfvén waves do not involve compression.

The other waves are *magnetosonic waves* which are nonlinear waves in the Riemann problem. The typically have shock or rarefaction wave solutions. The two waves shown above are fast and slow magnetosonic wave. The magnetosonic waves involve compression of the gas. Overall $c_\mathrm{f} \geq c_\mathrm{A} \geq c_\mathrm{s}$.

15 Diffusion and Cosmic Rays

15.1 Cosmic Rays as a separate fluid

As mentioned earlier, highly relativistic particles have long mean free paths and might not be treated correctly with the fluid approach, which assumes the mean-free path to be much smaller than the size of a computational cell. However, in the interstellar medium ($B \sim \mu$G) and for CR with energies up to 10^6 GeV the gyroradii are of the order of 10^3 AU, which is smaller than the computational cells. The CRs can thus be treated as a second fluid, which needs to be evolved separately and coupled via the magnetic field and the pressure to the rest of the MHD equations.

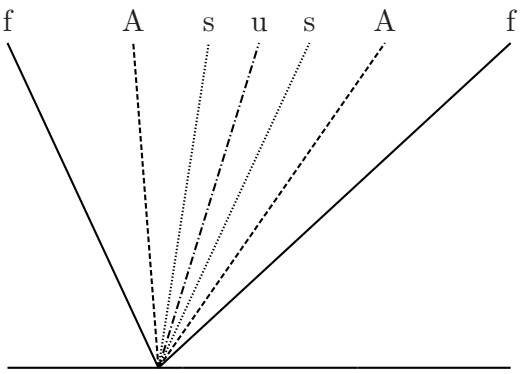

Figure 9: characteristics of the MHD problem including all MHD-waves.

15.2 CR in advection-diffusion approximation

The CRs which are coupled to the gas exert an additional pressure

$$p_{\rm CR} = (\gamma_{\rm CR} - 1) e_{\rm CR}, \tag{15.1}$$

where $\gamma_{\rm CR}$ is the adiabatic index for the CR and $e_{\rm CR}$ is the CR energy. For highly relativistic CRs $\gamma_{\rm CR} = 4/3$. However, we are only investigating the low-energy CRs and set $\gamma_{\rm CR} = 1.6$. The CRs therefore need to be added to the momentum and energy equations, where the CR and gas energy (pressure) add up to a total energy (pressure). In addition, the CRs can diffuse along the magnetic field lines, which means that the energy equation needs to be modified by a diffusion process. We solve the evolution of the energy separately for the CRs as well as for the total energy (gas plus CRs).

We describe the transport of CRs in the ISM with a diffusion-advection approximation

$$\partial_t e_{\rm CR} + \nabla(e_{\rm CR}\mathbf{v}) = -p_{\rm CR}\nabla\cdot\mathbf{v} + \nabla(\mathsf{K}\nabla e_{\rm CR}) + Q_{\rm CR}. \tag{15.2}$$

Here, $e_{\rm CR}$ is the CR energy density, $\mathbf{v}$ is the gas velocity, K is the CR diffusion tensor, and $Q_{\rm CR}$ is a CR source term, representing CR energy input. The diffusion is treated in an anisotropic way

$$\mathsf{K} \equiv K_{ij} = K_\perp \delta_{ij} + (K_\parallel - K_\perp) n_i n_j, \qquad n_i = \frac{B_i}{|\mathbf{B}|}, \tag{15.3}$$

with $K_\perp$ and $K_\parallel$ being the diffusion coefficients perpendicular and parallel to the direction of the magnetic field.

15.3 Extension to many CR energy bins

The general approach described above combines all the CR energy in one energy bin. However, as the CR diffusion coefficient depends on the energy of the CRs it is desirable to not just follow the total energy in CRs in one energy bin but split equation 15.2 into separate energy variables,

$$\partial_t e_{{\rm CR},i} + \nabla(e_{{\rm CR},i}\mathbf{v}) = -p_{{\rm CR},i}\nabla\cdot\mathbf{v} + \nabla(\mathsf{K}_i(e_{{\rm CR},i})\nabla e_{{\rm CR},i}) + Q_{{\rm CR},i}, \tag{15.4}$$

with different diffusion coefficients $\mathsf{K}(e_{{\rm CR},i})$. In our setup we use ten bins to split the CR energy. The total CR energy and pressure are then

$$e_{\rm CR} = \sum_1^{10} e_{{\rm CR},i} \tag{15.5}$$

$$p_{\rm CR} = \sum_i^{10} p_{{\rm CR},i}. \tag{15.6}$$

Using this splitting of the energy variables we are able to follow the CR spectrum self-consistently in space and time.

We assume the CR diffusion coefficient to have a functional form of $\mathsf{K} \propto e_{\rm CR}^{-0.3}$. The perpendicular component of the diffusion tensor is assumed to be 1% of the parallel diffusion coefficients.

$$p_{\rm tot} = p_{\rm th} + p_{\rm CR} + p_{\rm mag} \tag{15.7}$$
$$= (\gamma - 1)e_{\rm th} + (\gamma_{\rm CR} - 1)e_{\rm CR} + B^2/8\pi. \tag{15.8}$$

The closure relation for the system, the equation of state, combines the different contributions from CR and thermal pressure in an effective $\gamma_{\rm eff}$

$$\gamma_{\rm eff} = \frac{\gamma p_{\rm th} + \gamma_{\rm CR} p_{\rm CR}}{p_{\rm th} + p_{\rm CR}}. \tag{15.9}$$

The combined system of equations that we solve numerically is then given by

$$\frac{\partial \rho}{\partial t} + \nabla \cdot (\rho \mathbf{v}) = 0 \tag{15.10}$$
$$\frac{\partial \rho \mathbf{v}}{\partial t} + \nabla \cdot \left(\rho \mathbf{v}\mathbf{v} - \frac{\mathbf{B}\mathbf{B}}{4\pi} \right) + \nabla p_{\rm tot} = \rho \mathbf{g} \tag{15.11}$$
$$\frac{\partial e}{\partial t} + \nabla \cdot \left[(e + p_{\rm tot})\, \mathbf{v} - \frac{\mathbf{B}(\mathbf{B} \cdot \mathbf{v})}{4\pi} \right] = \rho \mathbf{v} \cdot \mathbf{g} + \nabla \cdot \mathsf{K} \nabla e_{\rm CR} \tag{15.12}$$
$$\frac{\partial \mathbf{B}}{\partial t} - \nabla \times (\mathbf{v} \times \mathbf{B}) = 0 \tag{15.13}$$
$$\frac{\partial e_{{\rm CR},i}}{\partial t} + \nabla (e_{{\rm CR},i} \mathbf{v}) = -p_{{\rm CR},i} \nabla \cdot \mathbf{v} + \nabla (\mathsf{K}_i \nabla e_{{\rm CR},i}) + Q_{{\rm CR},i} \qquad i \in 1..10. \tag{15.14}$$

15.4 Numerical treatment of CR in MHD simulations

Equation 15.2 can be written in the conservative form

$$\partial_t e_{\rm CR} + \nabla \cdot \mathbf{F}_{\rm CR,adv} + \nabla \cdot \mathbf{F}_{\rm CR,diff} = -p_{\rm CR} \nabla \cdot \mathbf{v} + Q_{\rm CR}. \tag{15.15}$$

The terms $-p_{\rm CR} \nabla \cdot \mathbf{v}$ and $Q_{\rm CR}$ are source terms, $\mathbf{F}_{\rm CR,adv} = e_{\rm CR}\mathbf{v}$ is the CR flux advected with the gas flow, $\mathbf{F}_{\rm CR,diff} = -\mathsf{K} \nabla e_{\rm CR}$ id the diffusive flux.

We solve the MHD equations using cell centered quantities for both the CR energy as well as the magnetic field quantities, $\mathbf{B}$. This approach is different from the numerical scheme used in other codes, where they use staggered mesh with the magnetic field components stored at face centres. In order to solve the combined system including CRs, we introduce a new energy equation for the $e_{\rm CR}$.

15.5 Anisotropic diffusion

The diffusion of CR shows a strong dependence on the direction of the magnetic field and needs to be treated in an anisotropic way parallel and perpendicular to the magnetic field lines. The diffusion tensor K thus depends on the variable magnetic field configuration. We now focus on the diffusion term of the advection-diffusion equation

$$\partial_t e_{\rm CR} + \nabla \cdot \mathbf{F}_{\rm CR} = 0, \qquad \mathbf{F}_{\rm CR} = -\mathsf{K} \nabla e_{\rm CR}. \tag{15.16}$$

Discretized, the complete three-dimensional conservation law reads

$$e^{n+1}_{\rm CR,i,j,k} = e^{n}_{\rm CR,i,j,k} - \frac{\Delta t}{\Delta x} \left(F_{\rm CR,i+\frac{1}{2},j,k} - F_{\rm CR,i-\frac{1}{2},j,k} \right) \tag{15.17}$$
$$- \frac{\Delta t}{\Delta y} \left(F_{\rm CR,i,j+\frac{1}{2},k} - F_{\rm CR,i,j-\frac{1}{2},k} \right) \tag{15.18}$$
$$- \frac{\Delta t}{\Delta z} \left(F_{\rm CR,i,j,k+\frac{1}{2}} - F_{\rm CR,i,j,k-\frac{1}{2}} \right). \tag{15.19}$$

The quantities $e^{n+1}_{\mathrm{CR,i,j,k}}$ and $e^{n}_{\mathrm{CR,i,j,k}}$ are cell centered CR energy densities in cell i, j, k at time steps t^{n+1} and t^n, and $F_{\mathrm{CR,i+\frac{1}{2},j,k}}, F_{\mathrm{CR,i-\frac{1}{2},j,k}}$ are the fluxes of CR through the left and right boundaries of the cell in x direction.

We can now combine the diffusion of CRs in a directionally split scheme to compute the total change in CR energy density. We subsequently apply the energy fluxes in x, y, and z direction

$$e^{n+b}_{\mathrm{CR,i,j,k}} = e^{n+a}_{\mathrm{CR,i,j,k}} - \frac{\Delta t}{\Delta x}\left(F_{\mathrm{CR,i+\frac{1}{2},j,k}} - F_{\mathrm{CR,i-\frac{1}{2},j,k}}\right) \tag{15.20}$$

$$e^{n+c}_{\mathrm{CR,i,j,k}} = e^{n+b}_{\mathrm{CR,i,j,k}} - \frac{\Delta t}{\Delta x}\left(F_{\mathrm{CR,i,j+\frac{1}{2},k}} - F_{\mathrm{CR,i,j-\frac{1}{2},k}}\right) \tag{15.21}$$

$$e^{n+1}_{\mathrm{CR,i,j,k}} = e^{n+c}_{\mathrm{CR,i,j,k}} - \frac{\Delta t}{\Delta x}\left(F_{\mathrm{CR,i,j,k+\frac{1}{2}}} - F_{\mathrm{CR,i,j,k-\frac{1}{2}}}\right) \tag{15.22}$$

with $e^{n+a}_{\mathrm{CR,i,j,k}}$ being the CR energy density after the advection step.

15.6 Time step limitations

As we are using an explicit scheme for the diffusion we have to obey stability criteria for the numerical scheme. The time step limitations for the diffusion part of the CR advection-diffusion equation is

$$\Delta t = 0.5\,\mathrm{CFL_{CR}}\,\frac{\min(\Delta x, \Delta y, \Delta z)^2}{K_{\parallel} + K_{\perp}}, \tag{15.23}$$

where $\mathrm{CFL_{CR}}$ is the Courrant-Friedrichs-Lewi number for the CR diffusion scheme and Δx, Δy, and Δz are the cell sizes.